Defence Research and Development Canada
Recherche et développement pour la défense Canada

DEFENCE R&D DÉFENSE

Maximum Likelihood Based ESM/Radar Track Association Algorithm in a New Modified Polar Coordinate

Yifeng Zhou, Winston Li and Henry Leung

Defence R&D Canada – Ottawa
TECHNICAL MEMORANDUM
DRDC Ottawa TM 2004-255
December 2004

Canada

Maximum Likelihood Based ESM/Radar Track Association Algorithm in a New Modified Polar Coordinate

Yifeng Zhou
DRDC Ottawa

Winston Li* and *Henry Leung
Department of Electrical and Computer Engineering, University of Calgary

Defence R&D Canada - Ottawa

Technical Memorandum

DRDC TM 2004-255

December 2004

Abstract

Association of radar and ESM tracks is an important component for multisensor-multitarget tracking systems. It is essential to the overall performance of a track fusion process. In this report, we present an ESM/track association algorithm in a new modified polar coordinate (MPC) system. The algorithm is based on a theoretical performance analysis of ESM/radar track association techniques in the MPC. Formulas for computing the correct and false association probabilities with and without state estimation biases are derived. We also discuss the effect of the number of observable states on association performance. The proposed algorithm uses a maximum likelihood (ML) algorithm for estimating the target states, of which the observable state estimates are subsequently used for the ESM/radar track association. Computer simulations are used to demonstrate the performance and improvement of the proposed ESM/radar track association method.

Résumé

L'association de pistes radar et SME est une composante importante des systèmes multicapteurs de poursuite de cibles multiples. Cette association est essentielle au rendement global du processus de fusion de pistes. Dans le présent document, nous présentons un algorithme d'association de pistes SME/radar dans un nouveau système de coordonnées polaires modifié (MPC). L'algorithme est basé sur une analyse de rendement théorique des techniques d'association de pistes SME/radar dans le système MPC. Les formules servant à calculer les probabilités d'association correctes et erronées avec et sans les biais d'estimation d'état sont dérivées. Nous discutons également des effets d'un bon nombre d'états observables sur le rendement de l'association. L'algorithme proposé utilise un algorithme de maximum de vraisemblance (MV) pour estimer les états des cibles. Ces états observables estimés sont ensuite utilisés pour l'association de pistes SME/radar. Les simulations informatiques servent à démontrer le rendement et l'amélioration de la méthode d'association de pistes SME/radar.

This page intentionally left blank.

Executive summary

This report focuses on the integration of radar and electronic support measures (ESM) sensors, in particular, the association of ESM/radar tracks. The work is motivated by the requirement of the DRDC TDP SISWS (Shipborne Integration of Sensor & Weapon System) project, and may contribute to the sensor manager part of the project in the future.

Fusion of target tracks from multiple similar or dissimilar sensors is an effective method to improve tracking accuracy and target acquisition rates. ESM sensor and radar are the two most popular types of sensors that have been deployed in air, sea and land surveillance systems. The information obtained by radar and ESM sensors is complementary, and integrating radar and ESM sensor outputs will help to increase the likelihood of target acquisition and to improve the tracking quality.

Track association is a pre-requisite for ESM/radar fusion and is essential to the overall performance of tracking systems. One of the uniqueness of ESM/radar track association is that the only common parameter between the ESM sensors and radar is the bearing measurements. In addition, the bearing measurements are not synchronized. Usually bearing-only tracking is required for ESM sensors for track association. However, bearing-only tracking usually suffers from the observability problem, i.e., the target states may not be observable when only bearing measurement is available. In order to make the all of the target states observable, it requires that the ESM sensor have a motion with non-zero derivative of higher order than the target, i.e., the platform has to maneuver more rapidly that the targets. This is a rare scenario in practice, especially for shipborne ESM sensors. Non-observable states will result in inaccurate and biased estimates, which in turn, will severely deteriorate the performance of ESM/radar track association.

In this report, we present ESM/track association algorithm in a new modified polar coordinate (MPC) system based on a theoretical performance analysis of ESM/radar track association techniques in the MPC. A conclusion from the performance analysis is that , under the Gaussian assumption, using more observable states would be able to improve the performance of ESM/radar association. In the proposed algorithm, a state vector is used which includes extra observable states in addition to the first three states in Aidala's MPC. The bearing-only tracking of the ESM sensors is implemented using a maximum likelihood (ML)

algorithm. Computer simulations show that the association performance can be improved effectively by using more observable states in the new MPC in different scenarios.

Y. Zhou, W. Li and H. Leung. 2004. Maximum Likelihood Based ESM/Radar Track Association Algorithm in a New Modified Polar Coordinate. DRDC Ottawa TM 2004-255. Defence R&D Canada - Ottawa.

Sommaire

Le présent document porte principalement sur l'intégration de capteurs radar et de capteurs mesure de surveillance électronique (MSE), et plus particulièrement sur l'association de pistes MSE/radar. Les travaux sont justifiés par les besoins du projet sur l'Intégration de capteurs et de systèmes d'armes embarqués (SISWS) du Programme de démonstration de technologies (TDP) de RDDC, et pourront servir plus tard à la partie du projet portant sur la gestion des capteurs.

La fusion de pistes de cibles provenant de plusieurs capteurs similaires ou différents est une méthode efficace pour augmenter la précision des poursuites et les taux d'acquisition de cibles. Les capteurs SME et radar sont les deux types de capteurs les plus utilisés, et ils sont déployés dans les systèmes de surveillance aérienne, maritime et terrestre. Les informations obtenues par les capteurs radar et SME sont complémentaires, et l'intégration des sorties des capteurs radar et SME aidera à augmenter la vraisemblance de l'acquisition de cibles et la qualité des poursuites.

L'association de pistes est un préalable à la fusion de pistes SME/radar, et elle est essentielle au rendement global des systèmes de poursuite. Une des spécificités de l'association de pistes SME/radar est que le seul paramètre commun entre les capteurs SME et radar est la mesure de gisement. De plus, les mesures de gisement ne sont pas synchronisées. Généralement, la poursuite en gisement seul est nécessaire pour les capteurs SME aux fins d'association de pistes. Toutefois, la poursuite en gisement seul est généralement touchée par le problème d'observabilité, c'est-à-dire que les états de cible peuvent ne pas être observables lorsqu'on dispose seulement des mesures de gisement. Afin que tous les états de cible soient observables, il faut que le capteur SME présente un mouvement avec une dérivée non nulle d'un ordre supérieur à celui de la cible, c'est-à-dire que la plate-forme doit se déplacer plus rapidement que la cible. Ce scénario est plutôt rare en pratique, particulièrement pour les capteurs SME de navire. Des états non observables résultent en estimations imprécises et faussées, qui à leur tour peuvent grandement détériorer le rendement de l'association de pistes SME/radar.

Dans le présent document, nous présentons un algorithme d'association de pistes SME/radar dans un nouveau système de coordonnées polaires modifié (MPC) basé sur une analyse de rendement théorique des techniques d'association de pistes SME/radar dans le

système MPC. La conclusion que nous pouvons tirer de l'analyse de rendement est que, selon l'assomption de Gauss, l'utilisation d'états plus observables permettrait d'améliorer le rendement de l'association de pistes SME/radar. Dans l'algorithme proposé, on utilise un vecteur d'état qui inclut des états observables supplémentaires en plus des trois premiers états du système MPC d'Aidala. La poursuite en gisement seul des capteurs SME est mise en application à l'aide d'un algorithme de maximum de vraisemblance (MV). Les simulations informatiques montrent que le rendement de l'association peut être amélioré de façon efficace si on utilise plus d'états observables avec le nouveau système MPC dans différents scénarios.

Y. Zhou, W. Li and H. Leung. 2004. Maximum Likelihood Based ESM/Radar Track Association Algorithm in a New Modified Polar Coordinate. DRDC Ottawa TM 2004-255. R & D pour la défense Canada - Ottawa.

Table of contents

List of figures

1. Introduction

Fusion of target tracks from multiple similar or dissimilar sensors is an effective method to improve tracking accuracy and target acquisition rates [1]. In practice, we are usually interested in fusing radar and electronic support measures (ESM) sensor outputs because of two reasons. First, radar and ESM sensors are the two most popular types of sensors that have been deployed in air surveillance systems [2]-[5]. Secondly, the outputs of radar and ESM sensors are complementary. Radar usually reports kinematics parameters of the targets (position, speed, acceleration with covariance information) while ESM sensors measure the attributes of the target emitters, which include information on emitter RF, PRI, PW as well as their bearings. The information obtained by radar and ESM sensors is complementary, and integrating radar and ESM sensor outputs will help to increase the likelihood of target acquisition and to improve the tracking quality. The overall outcome of fusion is improved situational awareness and more accurate and complete composite target track files.

In order to fuse radar and ESM sensor information, radar and ESM tracks need to be associated, i.e., tracks from the two sensors that represent the same emitter be recognized. It is a pre-requisite for ESM/radar fusion and essential to the overall performance of tracking systems. ESM/radar track association is unique in that the only common parameter between them is bearing measurement. In addition, the tracks from radar and ESM sensors are not synchronized in time because ESM tracks mainly depend on the illumination of the target emitters and the scheduling of the receivers. Since the only positional information that the ESM sensors observe is the bearing measurement, bearing-only tracking is required for ESM sensors for track association. The association performance follows closely that the bearing-only tracking at the ESM sensors. One issue with bearing-only tracking is the observability, i.e., the target states may not be observable when only bearing measurement is available. It was found that all the target dynamical states couldn't be estimated accurately when the targets are non-maneuvering. In recent years, many bearing-only tracking algorithms have been developed in the literature [6-12] to tackle the ovservability problem. The proposed approaches usually implement the bearing-only tracking in different coordinate systems including the polar coordinate (PC) [6-8], the Cartesian coordinate (CC) and the modified polar coordinate (MPC) [11]. The MPC approach by Aidala [11] has been shown to be able to overcome some shortcomings of passive tracking associated with the CC. In Aidala's

approach, the four states in the MPC are bearing rate, ratio of range rate and range, bearing, and inverse range. He showed that the bearing state is always observable, and the bearing rate and the ratio of range and range rate are observable almost everywhere except in some special cases. However, to make the inverse range observable, the sensor platforms or the targets must be maneuvering [13[-[16]. In [12], the performances of some track association methods based on bearing-only tracking in the CC and the MPC were compared using the computer simulations. In [9][17], theoretical performance was carried out for a multisensor track-to-track correlation technique in the CC, which includes the correct and false association probabilities.

In this report, we present an ESM/track association algorithm in a new modified polar coordinate (MPC) system. The algorithm is based on a theoretical performance analysis of ESM/radar track association techniques in the MPC. Note that the above-mentioned performance analysis is limited to particular state models used in the MPC and applicable to state vectors of fixed numbers of states. We develop a more general performance analysis, which is suitable for any number of states. In the analysis, correct and false association probabilities for maneuvering and non-maneuvering targets are derived. From the analysis, we show that the approach by Aidala always results in biased estimation of the fourth state, i.e., the inverse range, due to the non-observability for non-maneuvering targets and observers. The effect of the estimation bias of the inverse range state on the association performance is discussed. As a conclusion, we show that, under the Gaussian assumption, using more observable states can be used to improve ESM/radar association performance. To counter the observability of problem associated with non-maneuvering targets, we propose an approach in which the state vector includes extra observable states in addition to the first three states in Aidala's MPC. The state vector has five states, namely, bearing, ratio of range rate and range, bearing rate, heading direction, and ratio of target speed and range. The heading direction and the ratio of the target speed and range were first defined in [18][19] for linearly uniformly moving targets, and were shown to be observable almost everywhere except for an extreme condition. The bearing-only tracking of the ESM sensors is implemented using a maximum likelihood (ML) algorithm. The ESM/radar track association is then to convert the radar tracks to the new MPC and associate them with the ESM tracks. The CRB of the ML estimator is also derived. It should be mentioned that, when the targets or the observers are maneuvering, the additional observable states can still be used to improve the track association performance.

This report is organized as follows. In Section 2, we analyze the theoretical performance of classical ESM/radar track association techniques for maneuvering and non-maneuvering targets. The effect of the number of observable states on the association performance is also discussed. In Section 3, the system model for track association in the new MPC is introduced. Section 4 is devoted to the ML estimation method for ESM/radar sensor tracking and association algorithm proposed in the new MPC. Observability analysis for ESM bearing-only tracking in the new coordinate system is also given in this section. Finally, in Section 5, computer simulations are used to demonstrate the performance of the proposed track association algorithm.

2. Performance of Calssical ESM/Radar Track Association Techniques

In this section, we discuss the association performance for maneuvering and non-maneuvering targets. In particular, the effect of the number of observable states on association performance is discussed.

2.1 Association performance for manoeuvring and non-manoeuvring targets

Consider the near-constant velocity model. Using the Cartesian coordinate, the target state vector is given by $\boldsymbol{x}_{CC} = [x, \dot{x}, y, \dot{y}]^T$, where x and y are the positions, and $\dot{x}$ and $\dot{y}$ are the velocity along x- and y-axis, respectively. The MPC proposed by Aidala [11] is given by $\boldsymbol{x}_{MPC} = [\dot{\theta}, \dot{r}/r, \theta, 1/r]^T$, where $\dot{\theta}$, $\dot{r}/r$, θ, and $1/r$ represent the bearing rate, ratio of range rate and range, bearing, and inverse range, respectively. Assume that the target state estimates by radar and the ESM sensor are independent and Gaussian distributed with zero mean and variances given by

$$\sum_{radar} = diag\left[\delta^2_{\dot{\theta},radar}, \delta^2_{\dot{r}/r,radar}, \delta^2_{\theta,radar}, \delta^2_{1/r,radar}\right]$$

$$\sum_{ESM} = diag\left[\delta^2_{\dot{\theta},ESM}, \delta^2_{\dot{r}/r,ESM}, \delta^2_{\theta,ESM}, \delta^2_{1/r,ESM}\right],$$

respectively. Let us denote $\hat{\boldsymbol{x}}_{radar}$ and $\hat{\boldsymbol{x}}_{ESM}$ as the state estimates by radar and ESM sensor, respectively, the association is to determine whether they are from the same target or not. A statistical test for a four state vector can be written as

$$Y = \left(\hat{\boldsymbol{x}}_{radar} - \hat{\boldsymbol{x}}_{ESM}\right)^T \left(\sum_{radar} + \sum_{ESM}\right)^{-1} \left(\hat{\boldsymbol{x}}_{radar} - \hat{\boldsymbol{x}}_{ESM}\right). \quad (1)$$

The analysis can be categorized into four cases: (1) two tracks are from the same target and all target states are estimated unbiased; (2) two tracks are from the same target and one of the

states estimates is biased; (3) two tracks are from different targets and all target state estimates are unbiased; (4) two tracks are from different targets and one of the states is biased.

In the first case, the statistic *Y* can be shown to be chi-square-distributed with *n* degrees of freedom [20]

$$p_Y(y) = \frac{1}{2^{n/2}\Gamma(n/2)} y^{n/2-1} e^{-y/2}, \quad y \geq 0, \tag{2}$$

where *n* is the number of target states used for track association, and $\Gamma(q)$ is the gamma function

$$\begin{aligned} &\Gamma(q) = \int_0^\infty t^{q-1} e^{-t} dt, \quad q > 0, \\ &\Gamma(q) = (q-1)!, \quad q \text{ an integer}, q > 0, \\ &\Gamma(0.5) = \sqrt{\pi}, \Gamma(1.5) = 0.5\sqrt{\pi}. \end{aligned} \tag{3}$$

Let the test threshold be T . The correct and false association probability can be written as

$$p_c = \int_0^T p_Y(y) dy = \int_0^T \frac{1}{2^{n/2}\Gamma(n/2)} y^{n/2-1} e^{-y/2} dy, \tag{4}$$

and

$$p_f = \int_T^\infty p_Y(y) dy = 1 - p_c, \tag{5}$$

respectively. For even *n*, the correct association probability (4) can be simplified as

$$P_c = 1 - e^{-T/2} \sum_{k=0}^{n/2-1} \frac{1}{k!} \left(\frac{T}{2} \right)^k. \tag{6}$$

In the second case, assume that the *n*th state is unobservable with an estimation bias denoted by Δm_n . It is also assume that the rest (*n*-1) estimates are independently Gaussian distributed with zero mean. It can be verified that the *Y* follows a non-central chi-square distribution with *n* degrees of freedom

$$p_Y(y) = \frac{1}{2}\left(\frac{y}{\Delta m_n}\right)^{(n-2)/4} e^{-\left(y+\Delta m_n^2\right)/2} I_{n/2-1}\left(\sqrt{y}\Delta m_n\right),\ y \geq 0 \tag{7}$$

where $I_\alpha(x)$ denotes the α-th order modified Bessel function defined by

$$I_\alpha(x) = \sum_{k=0}^{\infty} \frac{(x/2)^{\alpha+2k}}{k!\Gamma(\alpha+k+1)},\quad x \geq 0\,. \tag{8}$$

The correct association probability can be obtained as

$$p_c = \int_0^T p_Y(y)dy = \int_0^T (1/2)\left(\frac{y}{\Delta m_n^2}\right)^{(n-2)/4} e^{-(y+\Delta m_n^2)/2} I_{n/2-1}(\sqrt{y}\Delta m_n)dy\,, \tag{9}$$

and the false association probability can be computed by (5).

In the third case, consider the normalized element $(\hat{x}_{radar,i} - \hat{x}_{ESM,i})^2 / \left(\delta_{radar,i}^2 + \delta_{ESM,i}^2\right)^{-1}$. It can be verified that, under the Gaussian assumption, the normalized element has a variance of unity. Assuming that the normalized element has a mean denoted by m_i, the statistics *Y* can be verified to follow a non-central chi-square distribution with *n* degrees of freedom

$$p_Y(y) = \frac{1}{2}\left(\frac{y}{q_n^2}\right)^{(n-2)/4} e^{-(y+q_n^2)/2} I_{n/2-1}(\sqrt{y}q_n),\quad y \geq 0 \tag{10}$$

where

$$q_n^2 = \sum_{i=1}^{n} m_i^2\ . \tag{11}$$

The correct and the false association probability are given by

$$p_c = \int_T^{\infty} p_Y(y)dy = \int_T^{\infty} (1/2)\left(\frac{y}{q_n^2}\right)^{(n-2)/4} e^{-(y+q_n^2)/2} I_{n/2-1}(\sqrt{y}q_n)dy \ , \tag{12}$$

and

$$p_f = \int_0^T p_Y(y)dy = 1 - p_c \ , \tag{13}$$

respectively.

In the fourth case, the tracks are from different targets and the estimate of the *n*th state has a bias Δm_n. The correct and the false association probability can be computed by (12) and (13), respectively, with q_n^2 given by

$$q_n^2 = \sum_{i=1}^{n-1} m_i^2 + (m_n + \Delta m_n)^2 \ . \tag{14}$$

2.2 Effect of number of observable states on association performance

When a target state is unobservable, its estimate will be biased. A biased state estimate will, in turn, deteriorate the association performance in terms of correct association probabilities. Most association algorithms have been based on the use of the observable state. Obviously, the use of different coordinate systems has an impact on the performance of association. In the following, we discuss how the number of observable states would affect the performance of association.

Consider different sets of observable states for ESM/radar track association. When only the bearing is used for association, the statistical test variable *Y* is chi-square distributed with a degree of freedom of one. Let T_1 denote the testing threshold. When more observable states are used, the new test variable can be written as

$$Y = \frac{1}{n}\left(\hat{\boldsymbol{x}}_{radar} - \hat{\boldsymbol{x}}_{ESM}\right)^T \left(\sum_{radar} + \sum_{ESM}\right)^{-1} \left(\hat{\boldsymbol{x}}_{radar} - \hat{\boldsymbol{x}}_{ESM}\right), \tag{15}$$

which can be verified to be a chi-square random variable with zero mean and variance 1/*n*. If the same test threshold T_1 is used, the correct association probability, assuming that the tracks are from the same target, is given by

$$p_c = \int_0^{T_1} p_Y(y)dy = \int_0^{T_1} \frac{1}{(1/n)^n 2^{n/2}\Gamma(n/2)} y^{n/2-1} e^{-yn/2} dy \,. \tag{16}$$

For an integer $l = n/2$, (16) can be written in a simpler form as

$$p_c = 1 - e^{-T_1 n/2} \sum_{k=0}^{l-1} \frac{1}{k!} \left(\frac{T_1 n}{2} \right)^k . \tag{17}$$

From (17), it can be seen that, when the number *n* of the observable states increases, the correct association probability improves.

When the tracks are from different targets, it can be verified that *Y* is a non-central chi-square variable with a nonzero mean and variance 1/*n*. The false association probability is given by

$$p_f = \int_0^{T_1} P_Y(y)dy = \int_0^{T_1} \frac{n}{2} \left(\frac{y}{q_n^2} \right)^{(n-2)/4} e^{-\left(q_n^2 + y\right)n/2} I_{n/2-1}(\sqrt{y} n q_n) dy, \tag{18}$$

which depends on both the number of observable states *n* and q_n. The parameter q_n is determined by the ratio of the state difference and the state estimation variance. The probability difference of falsely associating tracks from different targets with (*n*+1) and *n* observable states can be expressed as

$$\begin{aligned} \Delta p_f = \int_0^{T_1} \Bigg\{ & \frac{n+1}{2} \left(\frac{y}{q_n^2 + m_{n+1}^2} \right)^{(n-1)/4} e^{-\left(q_n^2 + m_{n+1}^2 + y\right)(n+1)/2} I_{(n+1)/2-1}\left(\sqrt{y}(n+1)\sqrt{q_n^2 + m_{n+1}^2}\right) \\ & - \frac{n}{2} \left(\frac{y}{q_n^2} \right)^{(n-2)/4} e^{-\left(q_n^2 + y\right)n/2} I_{n/2-1}(\sqrt{y} n q_n) \Bigg\} dy, \end{aligned} \tag{19}$$

where m_{n+1} represents the ratio of the (n+1)th observable state difference for two tracks from different targets and the (n+1)th state estimation variance. There is no explicit formula for determining the value of m_{n+1} that satisfies $\Delta p_f < 0$. If m_{n+1} is large enough (as will be shown in the next section), the false association probability will decrease. Another criterion is defined here to describe the averaged correct association probability of associating tracks from the same target and from different targets,

$$p_c^{average} = (p_c + (1 - p_f))/2. \tag{20}$$

To ensure that p_c increases and p_f decreases at the same time when using one more observable state (i.e., the (n+1)th state), the ratio m_{n+1} of the (n+1) state difference and estimation variance must satisfy $\Delta p_f < 0$.

2.3 Simulation results

In this section, we use computer simulations to demonstrate the performance of classical ESM/radar track association techniques. Figure 1 shows the correct association probabilities when bearing/inverse range or the four states in Aidala's MPC under different cases. In Figure 1(a), the radar and ESM tracks are originated from the same target while in Figure 1(b) they are from different targets. When the observer is made to be optimally maneuvering [16], the four states are observable for bearing-only tracking by the ESM sensor. If the target and ESM sensor are not maneuvering, the inverse range is not observable and will result in an estimation bias. Figures 1(a) and (b) show the correct association probability p_c in the absence of bias for the inverse range, w = 0, when the tracks are from same/different targets, respectively. It is shown that the correct association probabilities deteriorate with the increase of the estimation bias w of the inverse range. Therefore, the unobservable states are not preferred for track association in the classical track association techniques.

Figure 2 shows the effect of the number of observable states on the performance of the ESM/radar track association techniques. The testing threshold is fixed at T = 3.84. From Figure 2(a), we can observe that, when the tracks are from the same target, the correct association probability increases when extra observable states are used. Figure 2(b) shows the

false association probability versus the ratio of the (n+1)th state difference and estimation variance (n = 1 here). The ratio of the first state difference and estimation variance is given by $m_1^2 = 20$. When $m_2^2 > 7$, the false association probability is seen to decrease when an extra observable state is used. For small m_2^2, the false association probability increases with the number of the observable states. However, the correct association probability also increases when the tracks are from the same target and different targets. Figure 2(d) shows $\mathrm{sgn}(\Delta p_f)$ versus $i(=q_n^2)$ and $j(=m_{n+1}^2)$. Again n = 1. When the number of observable states and q_n^2 are fixed, it can be seen that the false association probability decreases when the ratio m_{n+1}^2 of the (n+1)th state difference and estimation variance is above certain value.

3. System Model for Track Association

In this section, we present a new modified polar coordinate in which ESM/radar track association is implemented. The observability of the system model is also discussed.

3.1 System model

The geometry of the new MPC is shown in Figure 3. The new MPC is a combination of Aidala's MPC and the polar coordinate proposed in [18][19]. It consists of the 5 states that are shown to be observable almost anywhere for non-maneuvering targets and observers. The state vector of the *k*th target is

$$\boldsymbol{X}_k(t_0) = [\theta_k(t_0),\ \dot{r}_k(t_0)/r_k(t_0), \dot{\theta}_k(t_0), \phi_k(t_0), v_k(t_0)/r_k(t_0)]^T, \qquad k = 1, 2, \cdots, K .$$

The first three states are defined in Aidala's MPC and the last two states are defined in the polar coordinate in [18][19]. When assuming a linearly uniform motion model for the target, the trajectory of the *k*th target can be written as [18]

$$\begin{bmatrix} x_k(t) \\ y_k(t) \end{bmatrix} = \begin{bmatrix} x_k(t_0) + (t - t_0)v_{kx} \\ y_k(t_0) + (t - t_0)v_{ky} \end{bmatrix}, \tag{21}$$

where $\{x_k(t), y_k(t)\}$ denotes the Cartesian coordinates of the target, and v_{kx} and v_{ky} are the target speeds along x- and y-axis, respectively. Aidala's MPC can be written as [11]

$$\theta_k(t) = \theta_k(t_0) + \tan^{-1}[s_3(t,t_0)/s_4(t,t_0)], \tag{22}$$

$$\dot{r}_k(t)/r_k(t) = \frac{s_1(t,t_0)s_3(t,t_0) + s_2(t,t_0)s_4(t,t_0)}{s_3^2(t,t_0) + s_4^2(t,t_0)}, \tag{23}$$

$$\dot{\theta}_k(t) = \frac{s_1(t,t_0)s_4(t,t_0) - s_2(t,t_0)s_3(t,t_0)}{s_3^2(t,t_0) + s_4^2(t,t_0)}, \tag{24}$$

where

$$s_1(t,t_0)=\dot{\theta}_k(t_0)+[1/r_k(t_0)][w_1(t,t_0)\cos\theta_k(t_0)-w_2(t,t_0)\sin\theta_k(t_0)]=\dot{\theta}(t_0),$$

$$s_2(t,t_0)=\dot{r}_k(t_0)/r_k(t_0)+[1/r_k(t_0)][w_1(t,t_0)\sin\theta_k(t_0)+w_2(t,t_0)\cos\theta_k(t_0)]=\dot{r}_k(t_0)/r_k(t_0),$$

$$s_3(t,t_0)=(t-t_0)\dot{\theta}_k(t_0)+[1/r_k(t_0)][w_3(t,t_0)\cos\theta_k(t_0)-w_4(t,t_0)\sin\theta_k(t_0)]=(t-t_0)\dot{\theta}(t_0),$$

$$s_4(t,t_0)=1+(t-t_0)[\dot{r}_k(t_0)/r_k(t_0)] \tag{25}$$

and

$$\begin{bmatrix} w_1(t,t_0) \\ w_2(t,t_0) \\ w_3(t,t_0) \\ w_4(t,t_0) \end{bmatrix}=\begin{bmatrix} \int_{t_0}^{t} a_{kx}(\lambda)d\lambda \\ \int_{t_0}^{t} a_{ky}(\lambda)d\lambda \\ \int_{t_0}^{t}(t-\lambda)ka_x(\lambda)d\lambda \\ \int_{t_0}^{t}(t-\lambda)a_{ky}(\lambda)d\lambda \end{bmatrix}=\boldsymbol{0} \tag{26}$$

for non-maneuvering targets and observers, a_{kx} and a_{ky} denote the relative acceleration of the *k*th target with respect to the ESM sensor. From (22) to (26), we have

$$\theta_k(t)=\theta_k(t_0)+\tan^{-1}\left[\frac{(t-t_0)\dot{\theta}_k(t_0)}{1+(t-t_0)[\dot{r}_k(t_0)/r_k(t_0)]}\right]. \tag{27}$$

Assume that $t=t_0+i\tau$ where τ is the sensor sampling time interval. For the new MPC, the following relationship also holds [18]

$$\theta_k(t)=\tan^{-1}\left\{\frac{\sin[\theta_k(t_0)]+i\tau[v_k(t_0)/r_k(t_0)]\cos[\phi_k(t_0)]}{\cos[\theta_k(t_0)]+i\tau[v_k(t_0)/r_k(t_0)]\sin[\phi_k(t_0)]}\right\}, \tag{28}$$

$$\phi_k(t)=\phi_k(t_0), \tag{29}$$

$$v_k(t)/r_k(t)=\frac{v_k(t_0)/r_k(t_0)}{\sqrt{1+2i\tau[v_k(t_0)/r_k(t_0)]\sin[\theta_k(t_0)+\phi_k(t_0)]+i^2\tau^2[v_k(t_0)/r_k(t_0)]^2}}. \tag{30}$$

We model the ESM sensor bearing measurement as

$$z_{k,esm}(t) = \theta_k(t) + n_{esm}(t) \tag{31}$$

where $n_{esm}(t)$ is the additive measurement noise which is assumed to be independently Gaussian distributed with zero mean. The radar measurement in the local CC is given by

$$\boldsymbol{z}_{k,radar}(t) = \boldsymbol{h}[\boldsymbol{x}_k(t)] + \boldsymbol{n}_{radar}(t) \tag{32}$$

where

$$\begin{aligned}
&\boldsymbol{x}_{k,radar}(t) = [x_k(t),\, \dot{x}_k(t),\, y_k(t),\, \dot{y}_k(t)]^T, \\
&\boldsymbol{h}[\boldsymbol{x}_k(t)] = \begin{bmatrix} h_1[\boldsymbol{x}_k(t)] \\ h_2[\boldsymbol{x}_k(t)] \end{bmatrix}, \\
&h_1[\boldsymbol{x}_k(t)] = \sqrt{x_k^2(t) + y_k^2(t)} = \sqrt{\left(x_k(t_0) + i\tau\dot{x}_k(t_0)\right)^2 + \left(y_k(t_0) + i\tau\dot{y}_k(t_0)\right)^2}, \\
&h_2(\boldsymbol{x}_k(t)) = \tan^{-1}\left[\frac{y_k(t_0) + i\tau\dot{y}_k(t_0)}{x_k(t_0) + i\tau\dot{x}_k(t_0)}\right].
\end{aligned} \tag{33}$$

Based on (32), we can estimate the target tracks in the CC by the maximum likelihood approach. The CC to the new MPC conversion can be done by

$$\begin{aligned}
&\theta_k(t) = \tan^{-1}\left(\frac{x_k(t)}{y_k(t)}\right), \\
&\dot{r}_k(t)/r_k(t) = \frac{\dot{x}_k(t)x_k(t) + \dot{y}_k(t)y_k(t)}{x_k^2(t) + y_k^2(t)}, \\
&\dot{\theta}_k(t) = \frac{\dot{x}_k(t)y_k(t) - x_k(t)\dot{y}_k(t)}{x_k^2(t) + y_k^2(t)}, \\
&\phi_k(t) = \tan^{-1}\left[\frac{\dot{y}_k(t)}{\dot{x}_k(t)}\right], \\
&v_k(t)/r_k(t) = \sqrt{\frac{\dot{x}_k^2(t) + \dot{y}_k^2(t)}{x_k^2(t) + y_k^2(t)}}.
\end{aligned} \tag{34}$$

Note that the states of the proposed MPC are not redundant because no state can be computed from the rest.

3.2 Observability analysis

We use the following rank condition matrix to test the observability of the target states

$$\boldsymbol{O} = \begin{bmatrix} \boldsymbol{O}_1 & \boldsymbol{0} \\ \boldsymbol{0} & \boldsymbol{O}_2 \end{bmatrix}, \tag{35}$$

where $\boldsymbol{O}_1$ can be obtained by the derivatives of $\theta_k(t)$ in Aidala's MPC with respect to its initial state

$$\begin{aligned} &\boldsymbol{O}_1(1, j) = 1, \\ &\boldsymbol{O}_1(2, j) = \frac{r_k(t_0)(j-1)\tau \cos(\theta_k(t_0 + (j-1)\tau) - \theta_k(t_0))}{r_k(t_0 + (j-1)\tau)}, \\ &\boldsymbol{O}_1(3, j) = -\frac{r_k(t_0)(j-1)\tau \sin(\theta_k(t_0 + (j-1)\tau) - \theta_k(t_0))}{r_k(t_0 + (j-1)\tau)}. \end{aligned} \tag{36}$$

and $\boldsymbol{O}_2$ can be obtained from the derivatives of the $\theta_k(t)$ definition in (28),

$$\boldsymbol{O}_2 = \begin{bmatrix} 1 & \dfrac{\partial \theta_k(t_0 + \tau)}{\partial \theta_k(t_0)} & \dfrac{\partial \theta_k(t_0 + 2\tau)}{\partial \theta_k(t_0)} \\ 0 & \dfrac{\partial \theta_k(t_0 + \tau)}{\partial (v_k(t_0)/r_k(t_0))} & \dfrac{\partial \theta_k(t_0 + 2\tau)}{\partial (v_k(t_0)/r_k(t_0))} \\ 0 & \dfrac{\partial \theta_k(t_0 + \tau)}{\partial \phi(t_0)} & \dfrac{\partial \theta_k(t_0 + 2\tau)}{\partial \phi_k(t_0)} \end{bmatrix}. \tag{37}$$

The matrix determinant of $\boldsymbol{O}_2$ is given by [18]

$$\det(\boldsymbol{O}_2) = \frac{-\tau\cos(\theta_k(t_0)+\phi_k(t_0))}{\xi_1(t_0)} \cdot \frac{-4\tau^2 - 2\tau(v_k(t_0)/r_k(t_0))\sin(\theta_k(t_0)+\phi_k(t_0))}{\xi_2(t_0)} + \frac{2\tau\cos(\theta_k(t_0)+\phi_k(t_0))}{\xi_2(t_0)} \cdot \frac{-\tau^2 - \tau(v_k(t_0)/r_k(t_0))\sin(\theta_k(t_0)+\phi_k(t_0))}{\xi_1(t_0)} \quad (38)$$

where

$$\xi_1(t_0) = (v_k(t_0)/r_k(t_0))^2 + \tau^2 + 2\tau(v_k(t_0)/r_k(t_0))\sin(\theta_k(t_0)+\phi_k(t_0)),$$
$$\xi_2(t_0) = (v_k(t_0)/r_k(t_0))^2 + 4\tau^2 + 4\tau(v_k(t_0)/r_k(t_0))\sin(\theta_k(t_0)+\phi_k(t_0)). \quad (39)$$

To guarantee $\det(\boldsymbol{O}_2) \neq 0$, the following condition must be satisfied,

$$\theta_k(t_0)+\phi_k(t_0) \neq \frac{\pi}{2}. \quad (40)$$

To guarantee $\det(\boldsymbol{O}_1) \neq 0$, the following condition must be satisfied,

$$\theta_k(t_0+iT) - \theta_k(t_0) \neq 0 \; or \; \frac{\pi}{2}. \quad (41)$$

It follows that the states in the new MPC are observable almost anywhere except under some very special conditions expressed as

$$\theta_k(t_0)+\phi_k(t_0) = \frac{\pi}{2},$$
$$\theta_k(t_0+i\tau) - \theta_k(t_0) = 0 \; or \; \frac{\pi}{2}. \quad (42)$$

For maneuvering observers, since the states in the new MPC can be computed from the states in the CC, which are observable [9], they are observable.

4. Maximum Likelihood Estimator

In this section, we apply the ML algorithm for estimating the tracks in the new MPC for the ESM sensor. The CRBs for the estimates are derived. The ESM/radar association logic based on the state estimates and their respective CRBs is also discussed.

4.1 ML estimates and CRBs

Because the new MPC is a combination of Aidala's MPC and the polar coordinate in [18], we define two negative log likelihood functions separately. The first is based on the ESM sensor measurement model (1) and bearing definition (27) in Aidala's MPC

$$L_1 = N\log(\pi\delta_{esm}^2) + \frac{1}{\delta_{esm}^2}\sum_{i=1}^{N}\left(z_{esm}(t_0 + i\tau) - \theta_k(t_0) - \tan^{-1}\left[\frac{i\tau\dot{\theta}_k(t_0)}{1 + i\tau[\dot{r}_k(t_0)/r_k(t_0)]}\right]\right)^2 . \quad (43)$$

where the constant terms are ignored. The second likelihood is based on the ESM sensor measurement equation (28) and bearing definition (25) in the polar coordinate of [18]

$$\begin{aligned} L_2 &= N\log(\pi\delta_{esm}^2) + \frac{1}{\delta_{esm}^2}\sum_{i=1}^{N}\left(z_{esm}(t_0 + i\tau) - \theta_k(t_0 + i\tau)\right)^2 \\ &= N\log(\pi\delta_{esm}^2) + \frac{1}{\delta_{esm}^2}\sum_{i=1}^{N}\Big(z_{esm}(t_0 + i\tau) \\ &\quad - \tan^{-1}\left\{\frac{\sin[\theta_k(t_0)] + i\tau[v_k(t_0)/r_k(t_0)]\cos[\phi_k(t_0)]}{\cos[\theta_k(t_0)] + i\tau[v_k(t_0)/r_k(t_0)]\sin[\phi_k(t_0)]}\right\}\Big)^2 . \end{aligned} \quad (44)$$

It can be verified that minimizing L_1 and L_2 is equivalent to minimizing

$$J_1 = \sum_{i=1}^{N}\left(z_{esm}(t_0 + i\tau) - \theta_k(t_0) - \tan^{-1}\left[\frac{i\tau\dot{\theta}_k(t_0)}{1 + i\tau[\dot{r}_k(t_0)/r_k(t_0)]}\right]\right)^2 \quad (45)$$

and

$$J_2 = \sum_{i=1}^{N} \left(z_{esm}(t_0 + i\tau) - \tan^{-1} \left\{ \frac{\sin[\theta_k(t_0)] + i\tau[v_k(t_0)/r_k(t_0)]\cos[\phi_k(t_0)]}{\cos[\theta_k(t_0)] + i\tau[v_k(t_0)/r_k(t_0)]\sin[\phi_k(t_0)]} \right\} \right)^2 . \quad (46)$$

Obviously, (45) and (46) are nonlinear optimization problems and numerical techniques are required. The Newton optimization method is used to estimate the *k*th target state $\boldsymbol{X}_k(t_0) = [\theta_k(t_0), \phi_k(t_0), \dot{\theta}_k(t_0), v_k(t_0)/r_k(t_0), \dot{r}_k(t_0)/r_k(t_0)]^T$. The (*p*+1)th iteration for calculating $\boldsymbol{X}_k(t_0)$ is given by

$$\boldsymbol{X}_{k,l}^{(p+1)}(t_0) = \boldsymbol{X}_{k,l}^{(p)}(t_0) - \mu^{(p)} \boldsymbol{H}_{k,l}^{-1} \boldsymbol{G}_{k,l} \quad (47)$$

where $\boldsymbol{X}_{k,1}(t_0) = [\theta_k(t_0), \dot{r}_k(t_0)/r_k(t_0), \dot{\theta}_k(t_0)]^T$, $\boldsymbol{X}_{k,2}(t_0) = [\phi_k(t_0), v_k(t_0)/r_k(t_0)]^T$, $\mu^{(p)}$ is the *p*th iteration step-size, $\boldsymbol{G}_{k,l}$ is the gradient vector given by

$$\boldsymbol{G}_{k,l} = 2\sum_{i=1}^{N} \boldsymbol{R}_{k,l}(i)\gamma_{kl}(i) \quad (48)$$

where

$$\gamma_{k,1}(i) = z_{esm}(t_0 + i\tau) - \hat{\theta}_k(t_0) - \tan^{-1}\left[\frac{i\tau\hat{\dot{\theta}}_k(t_0)}{1 + i\tau[\hat{\dot{r}}_k(t_0)/\hat{r}_k(t_0)]} \right],$$

$$\gamma_{k,2}(i) = z_{esm}(t_0 + i\tau) - \tan^{-1}\left\{ \frac{\sin[\hat{\theta}_k(t_0)] + i\tau[\hat{v}_k(t_0)/\hat{r}_k(t_0)]\cos[\hat{\phi}_k(t_0)]}{\cos[\hat{\theta}_k(t_0)] + i\tau[\hat{v}_k(t_0)/\hat{r}_k(t_0)]\sin[\hat{\phi}_k(t_0)]} \right\}, \quad (49)$$

and

$$\boldsymbol{R}_{k,l}(i) = \frac{\partial\theta_k(t_0 + i\tau)}{\partial\boldsymbol{X}_{k,l}(t_0)} . \quad (50)$$

Using the bearing definition in (27) in Aidala's MPC, we can compute $\boldsymbol{R}_{k,1}(i)$ by

$$\frac{\partial \theta_k(t_0 + i\tau)}{\partial \theta_k(t_0)} = 1,$$

$$\frac{\partial \theta_k(t_0 + i\tau)}{\partial (\dot{r}_k(t_0)/r_k(t_0)} = -\frac{(i\tau)^2 \hat{\dot{\theta}}_k(t_0)}{[i\tau \hat{\dot{\theta}}_k(t_0)]^2 + [1 + i\tau \hat{\dot{r}}_k(t_0)/\hat{r}_k(t_0)]^2},$$

$$\frac{\partial \theta_k(t_0 + i\tau)}{\partial \dot{\theta}_k(t_0)} = \frac{i\tau[1 + i\tau \hat{\dot{r}}_k(t_0)/\hat{r}_k(t_0)]}{[i\tau \hat{\dot{\theta}}_k(t_0)]^2 + [1 + i\tau \hat{\dot{r}}_k(t_0)/\hat{r}_k(t_0)]^2}. \quad (51)$$

$\boldsymbol{R}_{k,2}(i)$ can be calculated based on the bearing definition of (28) in the polar coordinate of [18] as

$$\frac{\partial \theta_k(t_0 + i\tau)}{\partial \phi_k(t_0)} = \frac{-i^2\tau^2 - i\tau[\hat{v}_k(t_0)/\hat{r}_k(t_0)]\sin[\hat{\theta}_k(t_0) + \hat{\phi}_k(t_0)]}{[\hat{v}_k(t_0)/\hat{r}_k(t_0)]^2 + i^2\tau^2 + 2i\tau[\hat{v}_k(t_0)/\hat{r}_k(t_0)]\sin[\hat{\theta}_k(t_0) + \hat{\phi}_k(t_0)]},$$

$$\frac{\partial \theta_k(t_0 + i\tau)}{\partial [v_k(t_0)/r_k(t_0)]} = \frac{-i\tau\cos[\hat{\theta}_k(t_0) + \hat{\phi}_k(t_0)]}{[\hat{v}_k(t_0)/\hat{r}_k(t_0)]^2 + i^2\tau^2 + 2i\tau[\hat{v}_k(t_0)/\hat{r}_k(t_0)]\sin[\hat{\theta}_k(t_0) + \hat{\phi}_k(t_0)]}. \quad (52)$$

We use the approximate Hessian

$$\boldsymbol{H}_{k,l} = \sum_{i=1}^{N} \boldsymbol{R}_{k,l}(i)\boldsymbol{R}_{k,l}^T(i). \quad (53)$$

The Fisher information matrix (FIM) of the ESM track estimates for the *k*th target, i.e., $\boldsymbol{X}_{k,1}(t_0) = [\theta_k(t_0), \dot{r}_k(t_0)/r_k(t_0), \dot{\theta}_k(t_0)]^T$ and $\boldsymbol{X}_{k,2}(t_0) = [\phi_k(t_0), v_k(t_0)/r_k(t_0)]^T$ can be written as

$$\boldsymbol{FIM}_{k,l} = \left(\delta_{esm}^2\right)^{-1} \sum_{i=1}^{N} \boldsymbol{R}_{k,l}(i)^T \boldsymbol{R}_{k,l}(i). \quad (54)$$

The CRB of $\boldsymbol{X}_k(t_0)$ is the diagonal elements of the inverse FIM,

$$CRB_{k,esm} = \begin{bmatrix} \boldsymbol{FIM}_{k,1}^{-1} & 0 \\ 0 & \boldsymbol{FIM}_{k,2}^{-1} \end{bmatrix}. \tag{55}$$

4.2 ML estimator and CRB for radar

The negative log likelihood function of the radar measurements can be written as

$$L = -\sum_{i=1}^{N} \ln\left(\frac{1}{2\pi\sqrt{\det(\boldsymbol{Q})}} \right) + \frac{1}{2}\sum_{i=1}^{N} \left[\boldsymbol{z}_{k,radar}(t_0 + i\tau) - \boldsymbol{h}(\boldsymbol{x}_k(t_0 + i\tau)) \right]^T \boldsymbol{Q}^{-1} \cdot \left[\boldsymbol{z}_{k,radar}(t_0 + i\tau) - \boldsymbol{h}(\boldsymbol{x}_k(t_0 + i\tau)) \right] \tag{56}$$

where

$$\boldsymbol{Q} = \begin{bmatrix} \delta_{r,radar}^2 & 0 \\ 0 & \delta_{\theta,radar}^2 \end{bmatrix}.$$

The target state $\boldsymbol{x}_{k,radar}(t_0)$ can be estimated similarly by using the Newton optimization method. When the radar tracks in the CC are estimated, they are converted into the new MPC using relationship (34). The Fisher Information matrix (*FIM*) can be written as

$$\boldsymbol{FIM}(\boldsymbol{x}_{k,radar}(t_0)) = \sum_{i=1}^{N} \begin{bmatrix} \dfrac{\partial h_1(x_k(t_0 + i\tau))}{\partial \boldsymbol{x}_k(t_0)} \\ \dfrac{\partial h_2(x_k(t_0 + i\tau))}{\partial \boldsymbol{x}_k(t_0)} \end{bmatrix}^T \begin{bmatrix} \delta_r^2 & 0 \\ 0 & \delta_\theta^2 \end{bmatrix}^{-1} \begin{bmatrix} \dfrac{\partial h_1(x_k(t_0 + i\tau))}{\partial \boldsymbol{x}_k(t_0)} \\ \dfrac{\partial h_2(x_k(t_0 + i\tau))}{\partial \boldsymbol{x}_k(t_0)} \end{bmatrix}. \tag{57}$$

The estimation covariance $\boldsymbol{W}$ of the state vector $\boldsymbol{x}_{k,radar}(t_0) = [x_k(t_0), \dot{x}_k(t_0), y_k(t_0), \dot{y}_k(t_0)]^T$ satisfies the following inequality

$$\boldsymbol{W} = E[\hat{\boldsymbol{x}}_{k,radar} - \boldsymbol{x}_{k,radar}][\hat{\boldsymbol{x}}_{k,radar} - \boldsymbol{x}_{k,radar}]^T \geq \boldsymbol{FIM}^{-1}(\boldsymbol{x}_{k,radar}). \tag{58}$$

The FIM of $\boldsymbol{X}_k(t)$ in the new MPC can be derived from the FIM of radar track in the CC as [10]

$$\begin{aligned}\boldsymbol{FIM}_{radar}(\boldsymbol{X}_k(t_0)) = \sum_{i=1}^{N}\left[\frac{\partial \boldsymbol{X}_k(t_0+i\tau)}{\partial \boldsymbol{x}_{k,radar}(t_0)}\right]^T \begin{bmatrix} \dfrac{\partial h_1(x_k(t_0+i\tau))}{\partial \boldsymbol{x}_k(t_0)} \\ \dfrac{\partial h_2(x_k(t_0+i\tau))}{\partial \boldsymbol{x}_k(t_0)} \end{bmatrix}^T \\ \cdot \begin{bmatrix} \delta_r^2 & 0 \\ 0 & \delta_\theta^2 \end{bmatrix}^{-1} \begin{bmatrix} \dfrac{\partial h_1(x_k(t_0+i\tau))}{\partial \boldsymbol{x}_k(t_0)} \\ \dfrac{\partial h_2(x_k(t_0+i\tau))}{\partial \boldsymbol{x}_k(t_0)} \end{bmatrix} \left[\frac{\partial \boldsymbol{X}_k(t_0+i\tau)}{\partial \boldsymbol{x}_{k,radar}(t_0)}\right].\end{aligned} \tag{59}$$

The CRB for $\boldsymbol{X}_k(t_0)$ is given by

$$CRB_{k,radar} = \left[\boldsymbol{FIM}_{radar}(\boldsymbol{X}_k(t_0)\right]^{-1}. \tag{60}$$

4.3 ESM/radar track association

Consider two tracks $\hat{\boldsymbol{X}}_{radar}$ and $\hat{\boldsymbol{X}}_{esm}$ by the ML estimators. Under the hypothesis that $\hat{\boldsymbol{X}}_{radar}$ and $\hat{\boldsymbol{X}}_{esm}$ are independent and Gaussian distributed, the association decision test is defined by

$$\left(\hat{\boldsymbol{X}}_{radar} - \hat{\boldsymbol{X}}_{esm}\right)\left(\boldsymbol{CRB}_{radar} + \boldsymbol{CRB}_{esm}\right)^{-1}\left(\hat{\boldsymbol{X}}_{radar} - \hat{\boldsymbol{X}}_{esm}\right)^T \le T \tag{61}$$

where T is a preset threshold. The radar and ESM tracks are said to be associated when (61) holds. Otherwise, they are considered to be from different targets. In practice, since the real target states are not known, we use the estimated target states and equations (54) and (60) to evaluate the CRB for the target state estimates in (61).

5. Experimental Results

In this section, we use computer simulations to assess the ESM/radar track association performance in the new MPC for different scenarios. These scenarios include: (1) a single target with locally linear dynamic model, (2) two close targets with locally linear dynamic models, which are moving away from the radar and ESM sensor, (3) two close targets with locally linear dynamic models, which are moving towards the sensors, (4) two close targets with locally linear dynamic models, which are moving away from the sensors, and (5) two targets with locally linear dynamic model, and the observers are maneuvering. In scenarios (1) to (4), the observers are assumed to be non-maneuvering.

Figure 4 compares the variances of the ML estimates of the ESM track with the CRBs. The initial position of the target is given by (-8000 *m*, 12000 *m*). The initial velocities along x- and y-axis are 320 *m*/*s* and 230 *m*/*s*, respectively. Figures 4(a) to 4(e) show the estimation errors of the five components of the state vector, respectively. It can be seen that the variances of the ML estimates of the ESM tracks approach their CRBs as the number of measurements increases.

Figure 5 and Figure 6 show the performance of different association algorithms using the proposed MPC with different testing thresholds. In Figure 5, the testing threshold *T* is set to 3.84 (corresponding to the correct association probability $p_c = 0.95$ for a chi-square distribution of freedom 1). Three association algorithms are compared. The first uses only one state (bearing) as in [6][8]. The second approach uses two states (bearing and range rate/range) and the third one combines all the five observable states in the new MPC. In Figure 5(a), the testing variable for a given number of samples, *k*, is defined as

$$Y = \left(\hat{\boldsymbol{X}}_{radar} - \hat{\boldsymbol{X}}_{esm} \right) \left(\boldsymbol{CRB}_{radar}(k) + \boldsymbol{CRB}_{esm}(k) \right)^{-1} \left(\hat{\boldsymbol{X}}_{radar} - \hat{\boldsymbol{X}}_{esm} \right)^{T}.$$

In Figure 5(a), the correct association probabilities with one, two, and five states are about 0.95, 0.98, and 0.995, respectively. The performance of the ESM/radar track association indeed improves with the use of more observable states. It is also observed that, when the number of measurements increases, both the target state estimation errors and the CRB

decrease while the correct association probability keeps almost the same. In Figure 5(b), the testing variable for *k* is defined as

$$Y = \left(\hat{\boldsymbol{X}}_{radar} - \hat{\boldsymbol{X}}_{esm} \right) \left(\boldsymbol{CRB}_{radar}(10) + \boldsymbol{CRB}_{esm}(10) \right)^{-1} \left(\hat{\boldsymbol{X}}_{radar} - \hat{\boldsymbol{X}}_{esm} \right)^{T}.$$

It can be seen that the correct association probability improves with the increase of the number of measurements because of the smaller estimation errors of $\left(\hat{\boldsymbol{X}}_{radar} - \hat{\boldsymbol{X}}_{esm} \right)$. In Figure 6, *T* is set to 2.05 (corresponding to a correct association probability $p_c = 0.85$ for a chi-square distribution of freedom 1).

Figure 7 shows the correct association probabilities of different association techniques when two targets are moving away from the observer. Both targets are observed by the radar and ESM sensor. The initial states of target A and target B are (-8000 *m*, 320 *m*/*s*, 12000 *m*, 230 *m*/*s*) and (-8000 *m*, 230 *m*/*s*, 10000 *m*, 320 *m*/*s*), respectively. *T* set to be 3.84. Let p_{caa} and p_{cbb} denote the probabilities of correctly associating ESM track A with radar track A, and ESM track B with radar track B, respectively, and p_{cab} and p_{cba} represent the probabilities of not associating ESM track A with radar track B, ESM track B with radar track A, respectively. The correct association probability in Figure 7(a) and 7(b) is defined as $p_c = (p_{caa} + p_{cbb} + p_{cab} + p_{cba})/4$. The definitions of the testing variable *Y* in Figure 7(a) and 7(b) are the same as in Figure 5(a) and 5(b), respectively. Figures 7 (a) and 7(b) show that the probability of correctly associating both the same target and different targets can be improved effectively by using more observable states. Another index for evaluating the performance of association is the probability of correctly associating the same target, which is defined as $p_c = (p_{caa} + p_{cbb})/2$, and shown in Figure 7(c) and 7(d). From Figure 7(c) and 7(d), we can observe than the probability of correctly associating the same target increases when more observable states are used.

Figure 8 shows the probabilities of falsely associating one target from another. The simulation parameters are the same as in Figure 7. The false association probability in Figure 8 is defined as $p_f = (p_{fab} + p_{fba})/2$, where p_{fab} and p_{fba} denote the probabilities of falsely associating ESM track A with radar track B, and ESM track B with radar Track A,

respectively. Figure 8 shows that the false association probabilities based on two states (bearing and heading direction) and five states are lower than that of the method based on bearing only. In Figures 7 and 8, it is shown that the two states and the five states based methods not only increase the probabilities of correctly associating tracks from the same target, but also decrease the probabilities of falsely associating tracks from different targets at the same time.

Figure 9 shows the correct association probabilities of different association techniques when two targets are moving towards the observers. The initial states of target A and B are (20000 *m*, 100 *m*/*s*, 30000 *m*, 200 *m*/*s*) and (20000 *m*, 150 *m*/*s*, 25000 *m*, 200 *m*/*s*), respectively. *T* is set to be 3.84. The correct association probability in Figure 9(a) and 9(b) is defined as $p_c = (p_{caa} + p_{cbb} + p_{cab} + p_{cba})/4$. The test *Y* in Figure 9(a) and 9(b) is the same as in Figure 5(a) and 5(b), respectively. In Figures 9 (a) and 9(b), it is shown that the probability of correctly associating both the same target and different targets improves effectively by using more observable states. The correct association probability in Figures 9(c) and 9(d) is defined as $p_c = (p_{caa} + p_{cbb})/2$. Figure 10 shows the probabilities of falsely associating one target from another. The simulation parameters are the same as in Figure 9. In this scenario, the false association probability decreases when more observable states are used.

Figure 11 shows the correct association probabilities for different association techniques when two close targets are moving away from the observers. The initial states of Target A and Target B are (*-8000 m*, *320 m*/*s*, *12000 m*, *230 m*/*s*) and *(-8000 m, 320 m/s, 11000 m, 230 m*/*s*), respectively. *T* is 3.84 for Figure 11(a) and 11(b), and is 2.05 for Figures 11(c) and 11(d). In Figure 11(a) and 7(c), the correct association probability is given by $p_c = (p_{caa} + p_{cbb} + p_{cab} + p_{cba})/4$. The test *Y* in Figure 11(a) and 11(b) is the same as in Figure 5(a) and 5(b), respectively. Figures 11(b) and 11(d) show that the probability of correctly associating the same target improves in the case of two close targets moving away from the observers. In Figures 11(a) and 11(b), it is observed that the total correct association probability $p_c = (p_{caa} + p_{cbb} + p_{cab} + p_{cba})/4$ decreases for small numbers of measurements when more observable states are used. However, it improves as the number of measurements increases. The five states based association becomes the best when the number of measurements is 70 for *T=3.84*, and 40 for the *T=2.05.*

Figure 12 shows the probabilities of falsely associating one target from another. The simulation parameters are the same as in Figure 11. In Figure 12(a) and 12(b), T is set to 3.84 and 2.05, respectively. When the number of measurements is small, it is observed that the false association probability increases with the use of extra observable states, which causes the deterioration of the total correct association probability shown in Figures 11(a) and 11(c). The reason is that the ratio of the state difference and estimation variance is small with small number of measurements. When the number of measurements increases, the probability of falsely associating two close targets approaches 0, and the total association probability with more states begin to its advantages. Although the false association probability may increases on its own, the probability of correctly associating the same target always improves with the use of extra observable states, as shown in Figures 11(b) and 11(d).

Figure 13 shows the correct association probabilities for maneuvering observers. The tracks of the targets and observers are shown in Figure 13(a). The correct association probabilities for different association techniques are shown in Figure 13(b). When the observer is maneuvering, the states of the targets in CC, i.e., positions and velocities along x- and y-axis are observable. We use an ML estimator, which is similar to that introduced in Section 5, for estimating the radar tracks in the CC. The estimated tracks are then converted to the new MPC for association. Figure 13(b) shows that the correct association probability improves with the use of extra observable states for maneuvering observers.

6. Conclusions

In this report, a new modified polar coordinate (MPC) system has been proposed based on a theoretical performance analysis of the classical track-to-track association techniques for maneuvering and non-maneuvering targets and observers. It is shown that the correct association probabilities will decrease with the introduction of bias into the observable states non-maneuvering targets and observers. The performance of the ESM/radar track association can be improved effectively if more observable states are used for association. Based on this conclusion, we proposed ESM/radar track association algorithm in the new MPC which includes extra observable states in addition to Aidala's MPC. A maximum likelihood (ML) algorithm is proposed to estimate the ESM tracks in the new MPC. The new MPC formulation is applicable to both maneuvering and non-maneuvering targets and observers. The CRBs of the radar and ESM track estimates are also derived. Computer simulations were used to demonstrate the performance of the proposed algorithm. It was shown that the track association performance improved effectively by using more observable states in the new MPC in different scenarios.

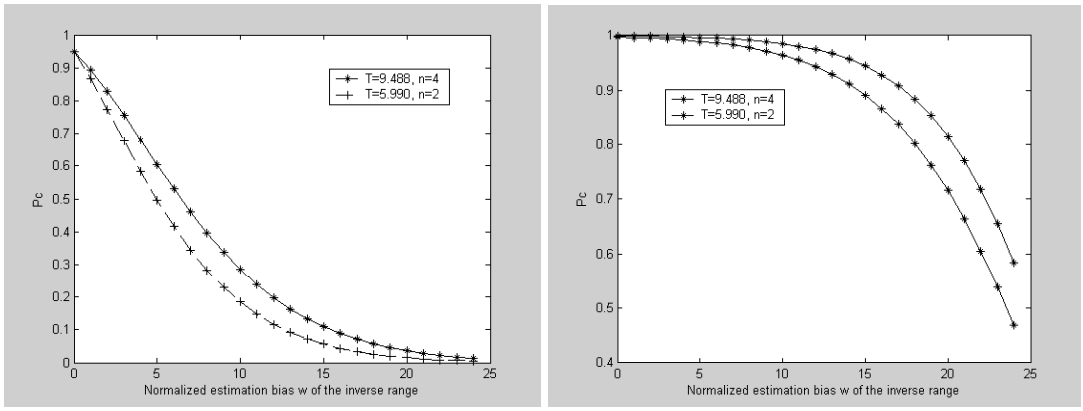

Figure 1. Figure 1. Correct association probabilities under different cases: (a) The radar and ESM tracks are related to the same target; (b) The radar and ESM tracks are related to different targets. The p_c *at* w *= 0 in (a) and (b) shows the correct association probability in case 1 and case 3, respectively, i.e. no estimation biases for the target states.*

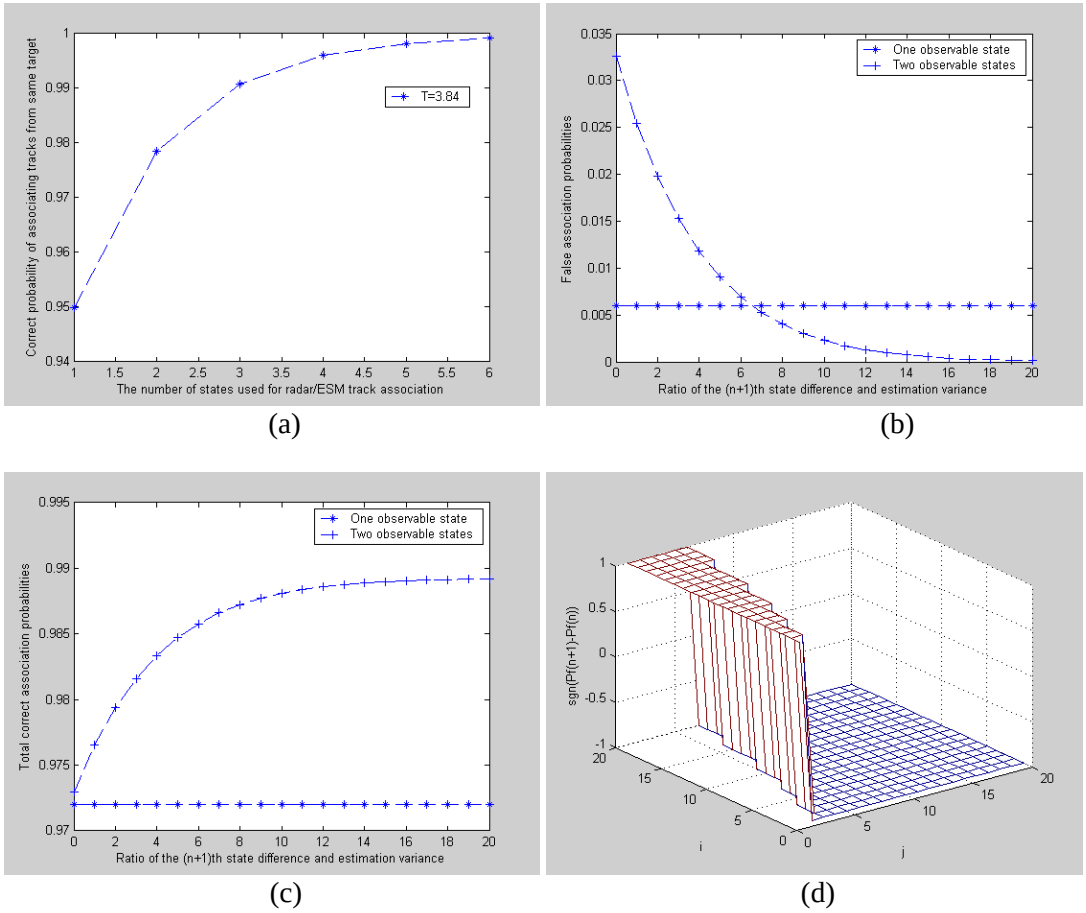

Figure 2. Association probability versus the number of observable states used for ESM/radar track association. The testing threshold is fixed to be T = 3.84. (a) probability of correctly associating tracks from the same target; (b) probability of falsely associating tracks from different targets; (c) probability of correctly associating tracks from the same targets and from different targets; (d) $\mathrm{sgn}(\Delta p_f)$ *versus* $i(=q_n^2)$ *and* $j(=m_{n+1}^2)$ *, n = 1 here.*

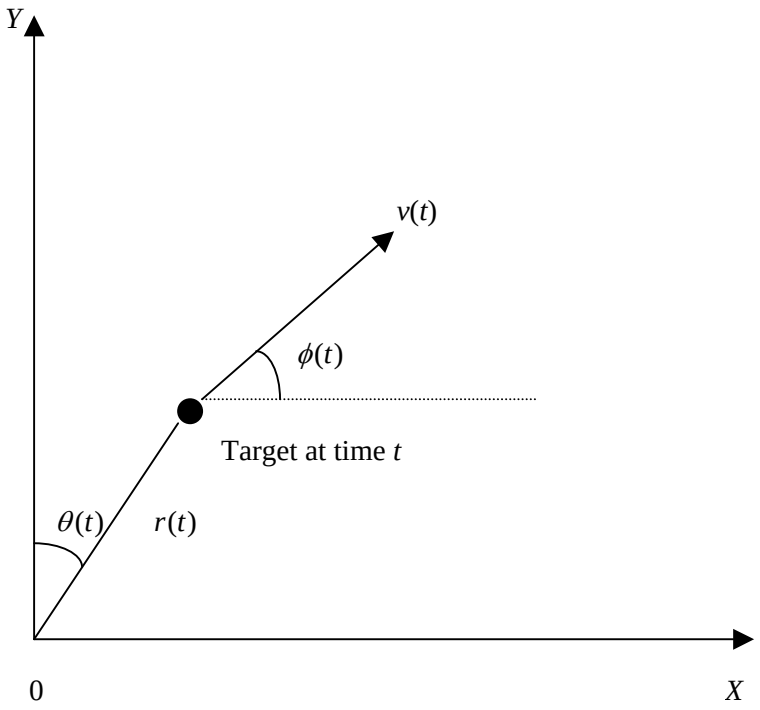

Figure 3. Geometry of the new MPC.

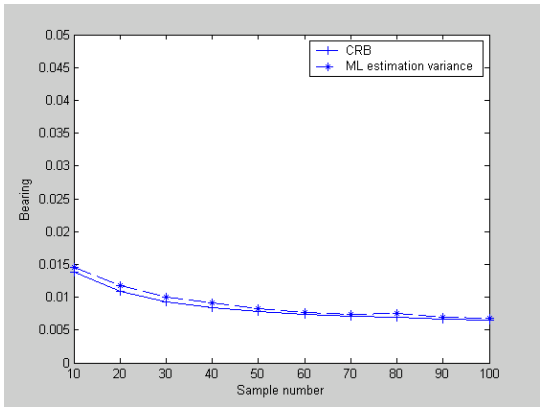

(a)

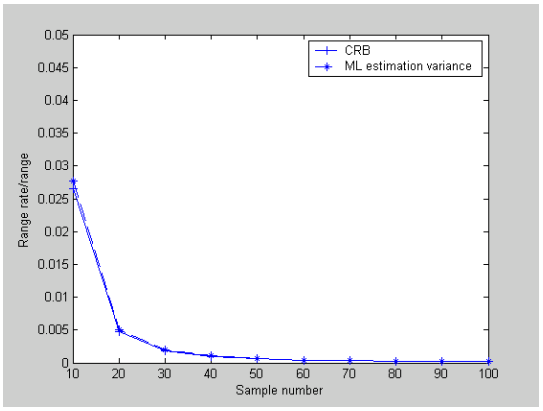

(b)

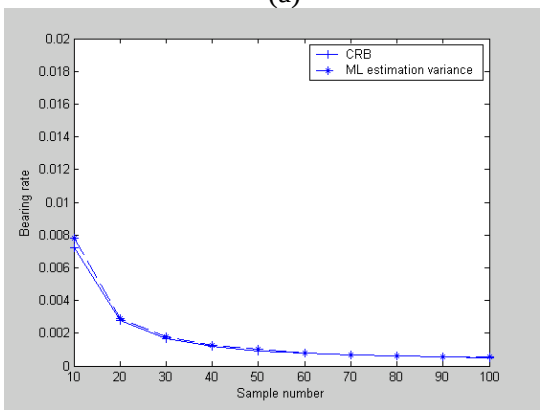

(c)

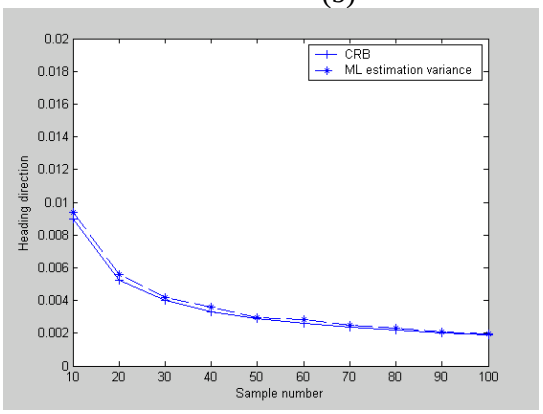

(d)

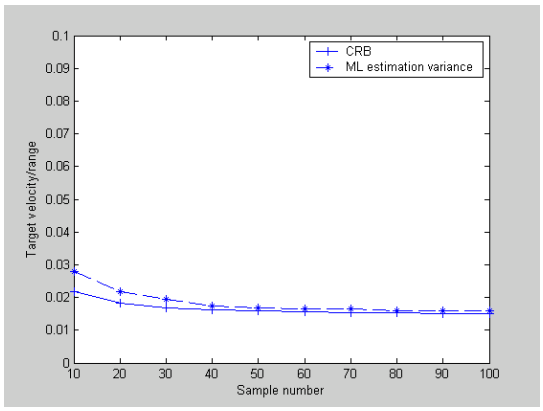

(e)

Figure 4. Comparison of the ML estimator and CRB for ESM tracking: (a) bearing; (b) range rate/range; (c) bearing rate; (d) heading direction; (e) target velocity/range.

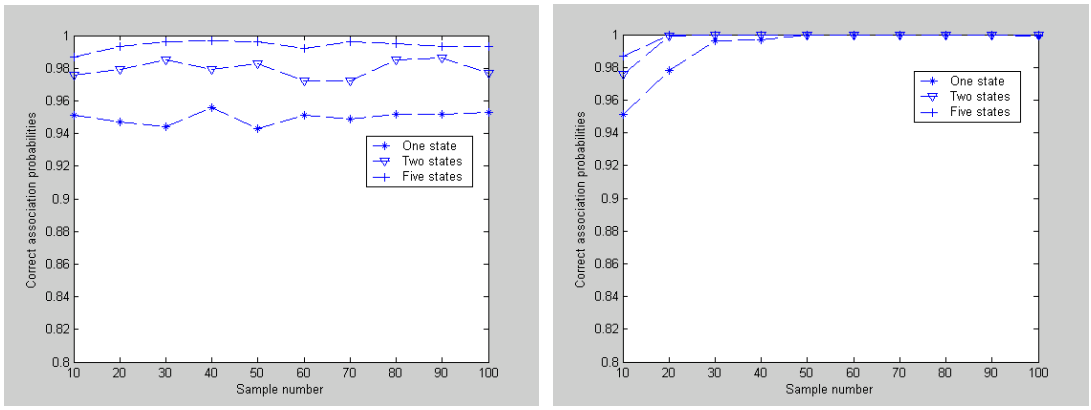

Figure 5. Correct association probability for the single target. The testing threshold is 3.84. (a) The variance in the testing variable changes with the sample number; (b) The variance in the testing variable is fixed.

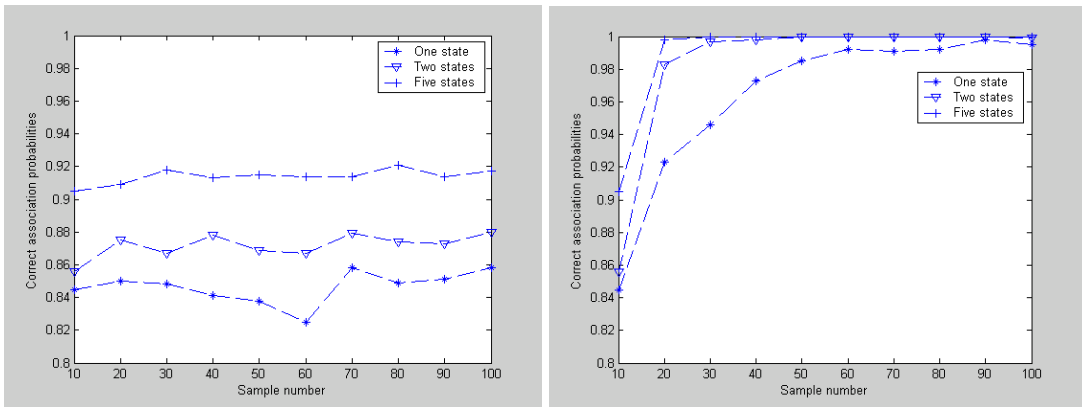

Figure 6. Correct association probability for the single target. The testing threshold is 2.05. (a) The variance in the testing variable changes with the sample number; (b) The variance in the testing variable is fixed.

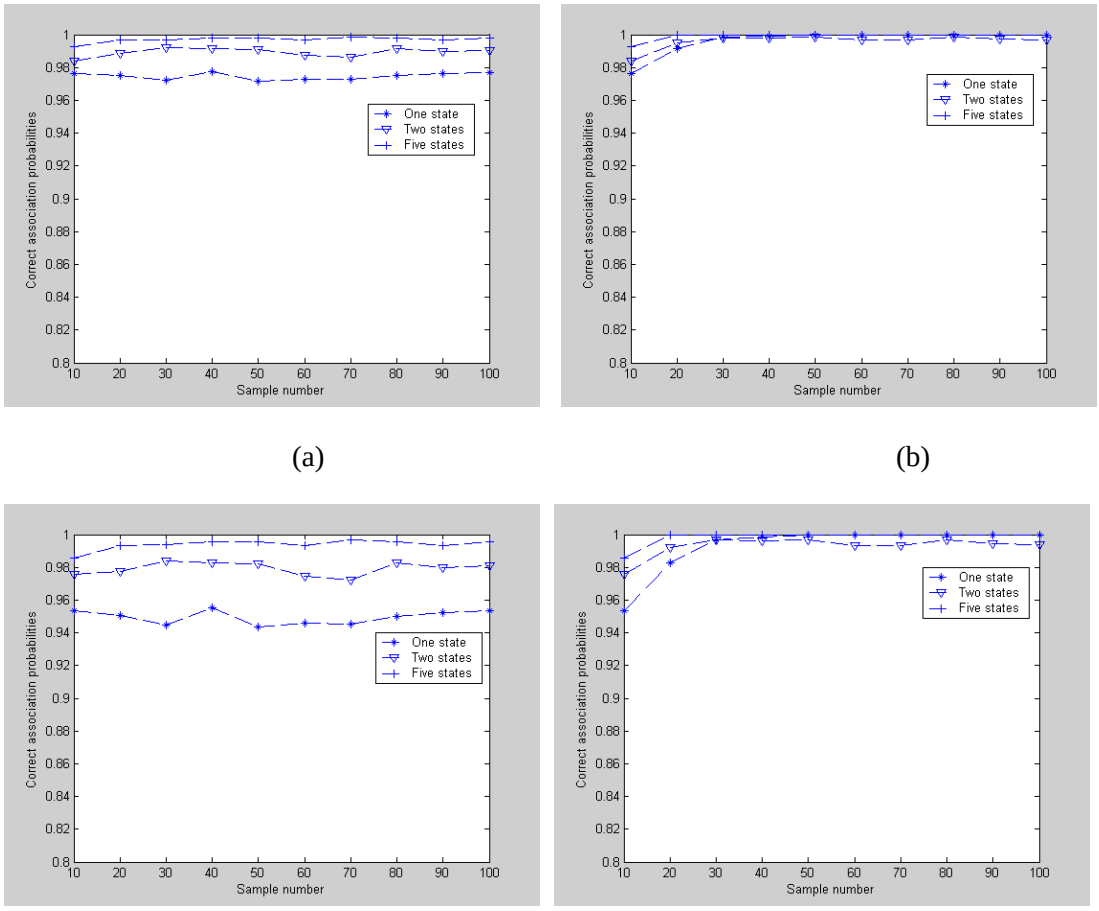

Figure 7. Correct association probabilities for two close targets moving away from the observer: (a) $p_c = (p_{caa} + p_{cbb} + p_{cab} + p_{cba})/4$*. Changed variance in the testing variable; (b)* $p_c = (p_{caa} + p_{cbb})/2$*; Fixed variance in the testing variable; (c)* $p_c = (p_{caa} + p_{cbb} + p_{cab} + p_{cba})/4$*. Changed variance in the testing variable; (d)* $p_c = (p_{caa} + p_{cbb})/2$*. Fixed variance in the testing variable.*

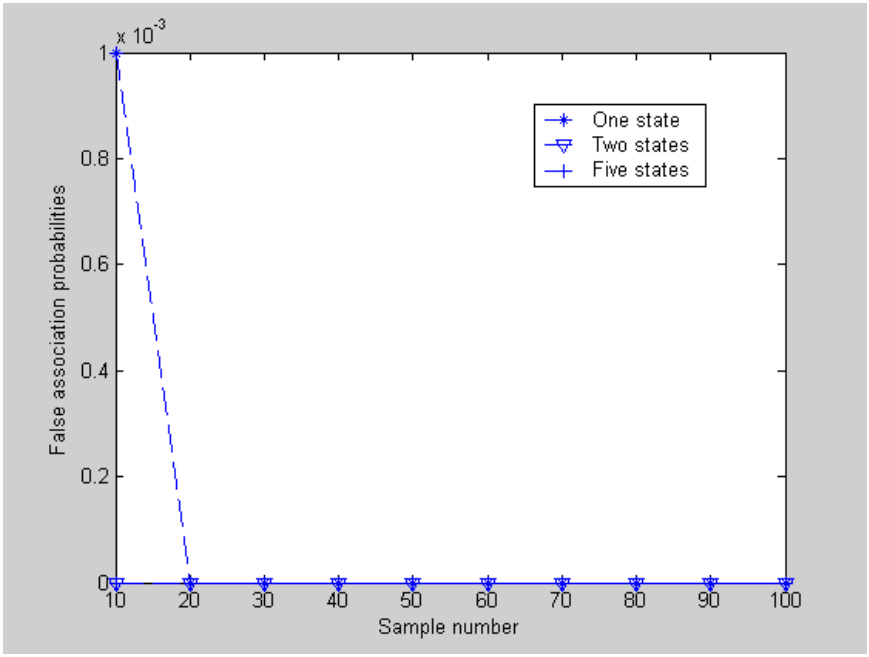

Figure 8. False association probabilities for the two targets in Figure 7.

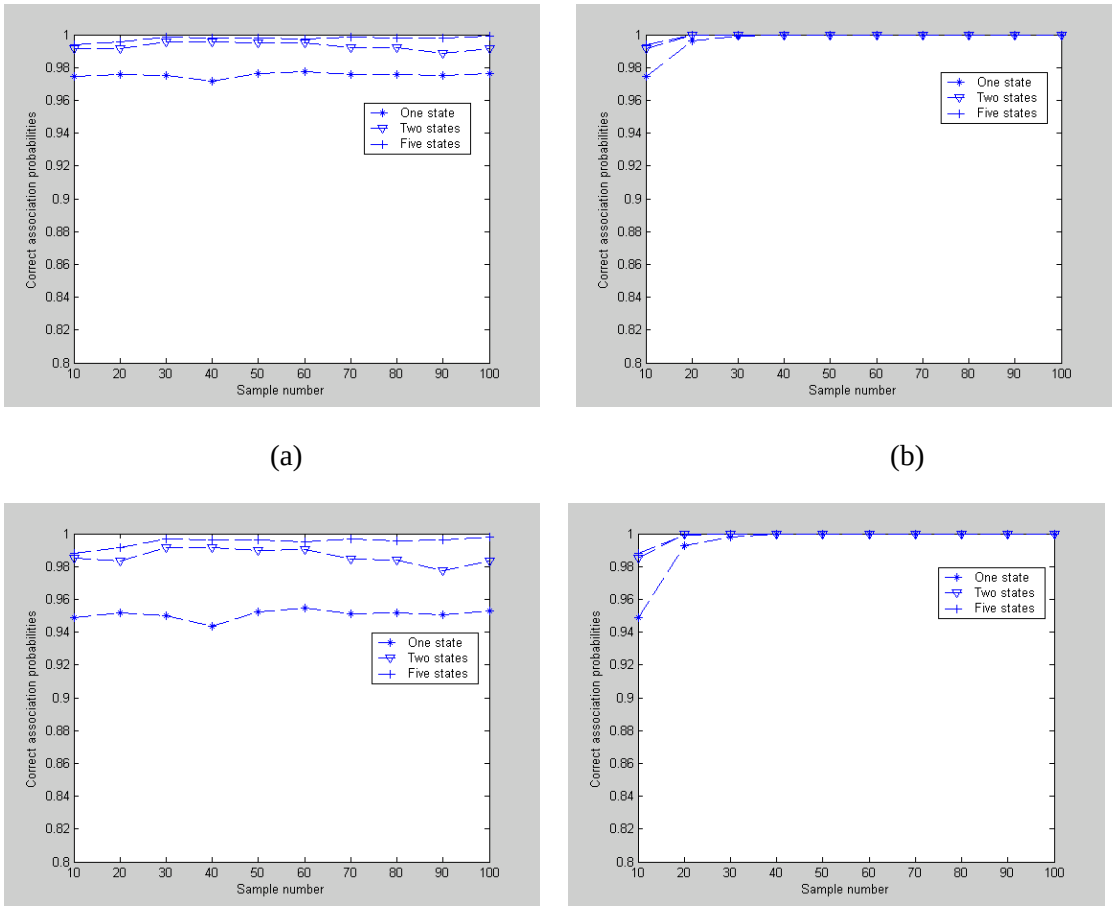

Figure 9. Correct association probabilities for two close targets moving toward the observer: (a) $p_c = (p_{caa} + p_{cbb} + p_{cab} + p_{cba})/4$*. Changed variance in the testing variable; (b)* $p_c = (p_{caa} + p_{cbb})/2$*; Fixed variance in the testing variable; (c)* $p_c = (p_{caa} + p_{cbb} + p_{cab} + p_{cba})/4$*. Changed variance in the testing variable; (d)* $p_c = (p_{caa} + p_{cbb})/2$*. Fixed variance in the testing variable.*

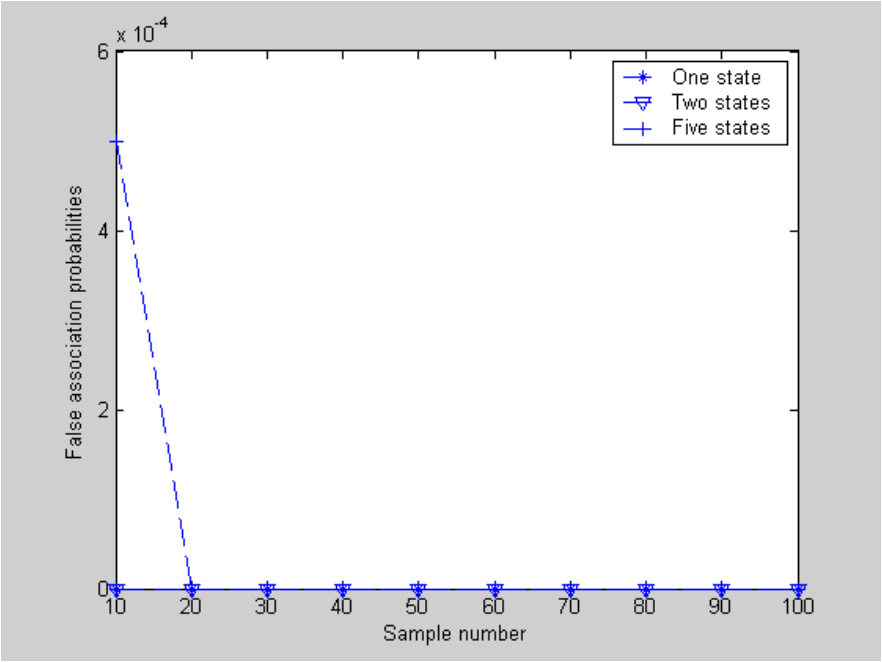

Figure 10. False association probabilities for the two targets in Figure 9.

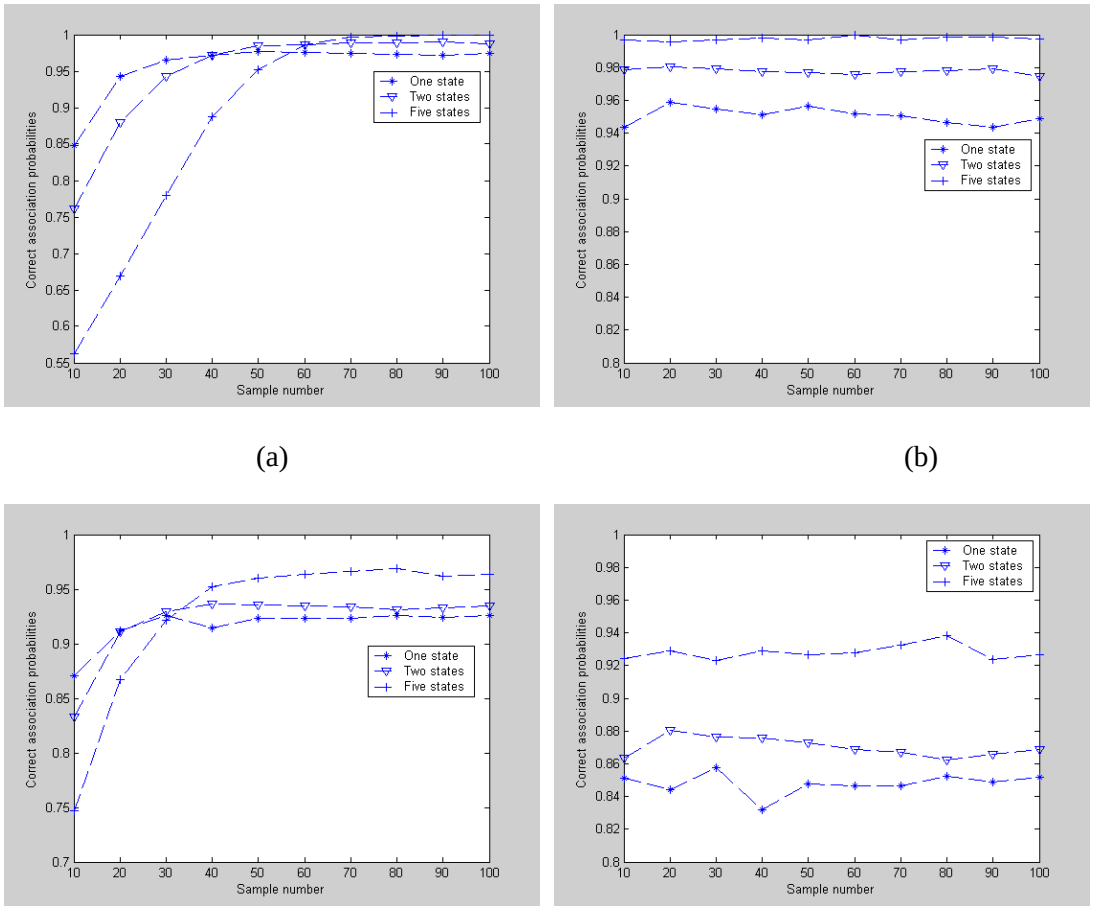

Figure 11. Correct association probabilities for two very close targets moving away from the observer: (a) T = *3.84,* $p_c = (p_{caa} + p_{cbb} + p_{cab} + p_{cba})/4$*; (b)* T = *2.05,* $p_c = (p_{caa} + p_{cbb})/2$.

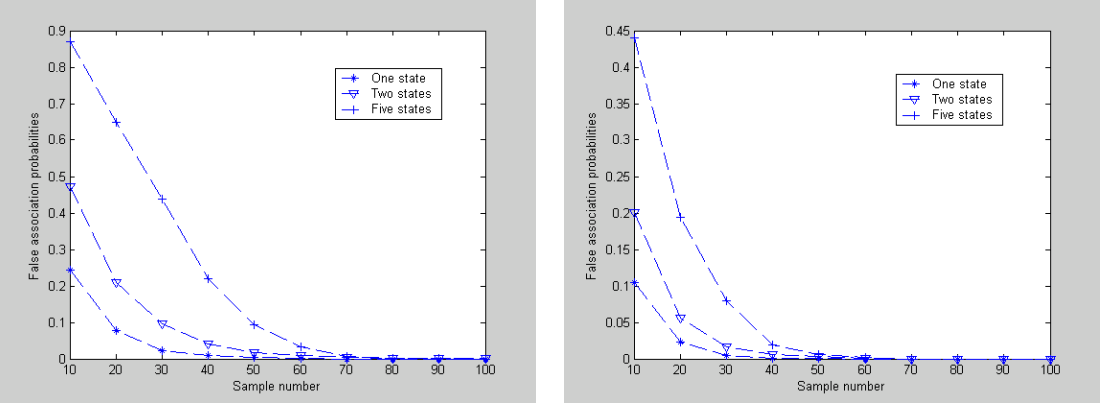

(a) (b)

Figure 12. False association probabilities for the two targets in Figure 11: (a) T = *3.84; (b)* T = *2.05.*

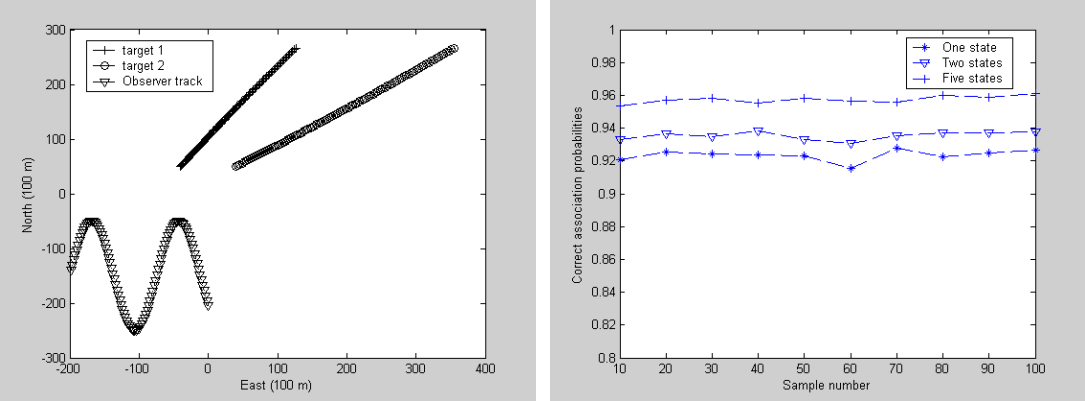

(a) (b)

Figure 13. Correct association probabilities for maneuvering observer: (a) tracks for targets and observers; (b) correct association probabilities.
$p_c = (p_{caa} + p_{cbb} + p_{cab} + p_{cba})/4$. *The testing threshold is 2.05.*

7. References

[1] S. Blackman and R. Popli, *Design and Analysis of Modern Tracking Systems*, Boston: Artech House, 1999

[2] S. Challa and G. W. Pulford, "Joint target tracking and classification using radar and ESM sensors", *IEEE Trans. Aerospace and Electronics Systems*, 37, no. 3, pp. 1039-1055, April 2001

[3] K. Kim, "Integration of an electronic support measures (ESM) and an alpha-beta radar tracker", *Proc. SPIE*, 1305, pp. 324-335, 1990

[4] G. A. Watson and W. D. Blair, "Revisit control of a phased-array radar for tracking maneuvering targets when supported by a precise electronic support measures (ESM) sensor", *Proc. SPIE*, 2235, pp. 448-459, 1990

[5] J. Couture, E. Boily and M. Simard, "Sensor data fusion of radar, ESM, IFF, and data LINK of the Canadian patrol frigate and the data alignment issues", *Proc. SPIE*, 2759, pp. 361-372, 1996

[6] G. V. Trunk and J. D. Wilson, "Association of DF bearing measurements with radar tracks", *IEEE Trans. Aerospace and Electronic Systems*, vol. 23, no. 4, pp. 438-447, July 1987

[7] H. Wang, S. Y. Mao, Y. He and Y. J. Liu, "Triple-threshold radar-to-ESM correlation algorithm when each radar track is specified by different number of measurements", *IEE Proc. Radar. Sonar Navig.*, vol. 147, no. 4, pp. 177-181, Aug. 2000

[8] J. F. Smith, "Fuzzy logic association: performance, implementation issues, and automated resource allocation", *Proc. SPIE*, 3720, pp. 228-236, 1990

[9] A. Farina and R. Miglioli, "Association of active and passive tracks for airborne sensors", *Signal Processing*, vol. 69, pp. 209-217, 1998

[10] B. F. La Scala and A. Farina, "Choosing a track association method", *Information Fusion*, vol. 3, pp. 119-133, 2002

[11] V. J. Aidala and S. E. Hammel, "Utilization of modified polar coordinates for bearing-only tracking", *IEEE Trans. Automatic Control*, vol. 28, no. 3, 283-294, 1983

[12] D. Gendron, K. Benameur and M. Farooq, "Track-to-Track fusion in a heterogeneous sensory environment", Proc. *4th International Conference on Information Fusion*, Montreal, Quebec, Canada, August 2001

[13] T. L. Song, “Observability of target tracking with bearing-only measurements”, *IEEE Trans. Aerospace and Electronic Systems*, vol. 32, no. 4, pp. 1468-1471, 1996

[14] J. P. Le Cadre and C. Jauffret, “Discrete-time observability and estimability analysis for bearing-only target motion analysis”, *IEEE Trans. Aerospace and Electronic Systems*, vol. 33, no. 1, pp. 178-201, 1997

[15] T. R. Kronhamn, “Bearings-only target motion analysis based on a multihypothesis Kalman filter and adaptive ownship motion control”, *IEE Proc. –Radar, Sonar Navig*., vol. 145, no. 4, no. 247-252, 1998

[16] J. M. Passerieux and D. vn Cappel, “Optimal observer maneuver for bearings-only tracking”, *IEEE Trans. Aerospace and Electronic Systems*, vol. 34, no. 3, pp. 777-788, 1998

[17] F. R. Castella, “Theoretical performance of a multisensor track-to-track correlation technique”, *IEE Proc. –Radar, sonar Navig*., vol. 142, no. 6, pp. 281-285, Dec. 1995

[18] Y. Zhou, P. C. Yip and H. Leung, “Tracking the direction-of-arrival of multiple moving targets by passive arrays: algorithm”, *IEEE Trans. Signal Processing*, vol. 47, no. 10, pp. 2655-2666, Oct. 1999

[19] Y. Zhou, P. C. Yip and H. Leung, “Tracking the direction-of-arrival of multiple moving targets by passive arrays: asymptotic performance analysis”, *IEEE Trans. Signal Processing*, vol. 47, no. 10, pp. 2644-2654, Oct. 1999

[20] A. Leon-Garcia, *Probability and Random Processes for Electrical Engineering*, Mass.: Addison-Wiley, 1994

[21] Y. Zhou, H. Leung and P. C. Yip, “An exact maximum likelihood registration algorithm for data fusion”, *IEEE Trans. Signal Processing*, vol. 45, no. 6, pp. 1560-1572, June 1997

[22] J. H. Taylor, “The Cramer-Rao estimation error lower bound computation for deterministic nonlinear systems”, *IEEE Trans. Automatic Control*, vol. 24, no. 2, pp. 343-344, April 1979

[23] T. W. Anderson, *An Introduction to Multivariate Statistical Analysis*, New York: Wiley, 1984

DOCUMENT CONTROL DATA

(Security classification of title, body of abstract and indexing annotation must be entered when the overall document is classified)

1. ORIGINATOR (the name and address of the organization preparing the document. Organizations for whom the document was prepared, e.g. Establishment sponsoring a contractor's report, or tasking agency, are entered in section 8.)

Defence R&D Canada – Ottawa
Ottawa, Ontario K1A 0Z4

2. SECURITY CLASSIFICATION (overall security classification of the document, including special warning terms if applicable)

UNCLASSIFIED

3. TITLE (the complete document title as indicated on the title page. Its classification should be indicated by the appropriate abbreviation (S,C or U) in parentheses after the title.)

Maximum Likelihood Based ESM/Radar Track Association Algorithm in a New Modified Polar Coordinate (U)

4. AUTHORS (Last name, first name, middle initial)

Yifeng Zhou, Winston Li and Henry Leung

5. DATE OF PUBLICATION (month and year of publication of document)	6a. NO. OF PAGES (total containing information. Include Annexes, Appendices, etc.)	6b. NO. OF REFS (total cited in document)
December 2004	49	23

7. DESCRIPTIVE NOTES (the category of the document, e.g. technical report, technical note or memorandum. If appropriate, enter the type of report, e.g. interim, progress, summary, annual or final. Give the inclusive dates when a specific reporting period is covered.)

DRDC Ottawa Technical Memorandum

8. SPONSORING ACTIVITY (the name of the department project office or laboratory sponsoring the research and development. Include the address.)

DRDC Ottawa

9a. PROJECT OR GRANT NO. (if appropriate, the applicable research and development project or grant number under which the document was written. Please specify whether project or grant)	9b. CONTRACT NO. (if appropriate, the applicable number under which the document was written)
13cr11	

10a. ORIGINATOR'S DOCUMENT NUMBER (the official document number by which the document is identified by the originating activity. This number must be unique to this document.)	10b. OTHER DOCUMENT NOS. (Any other numbers which may be assigned this document either by the originator or by the sponsor)
DRDC Ottawa TM 2004-255	

11. DOCUMENT AVAILABILITY (any limitations on further dissemination of the document, other than those imposed by security classification)

(x) Unlimited distribution
( ) Distribution limited to defence departments and defence contractors; further distribution only as approved
( ) Distribution limited to defence departments and Canadian defence contractors; further distribution only as approved
( ) Distribution limited to government departments and agencies; further distribution only as approved
( ) Distribution limited to defence departments; further distribution only as approved
( ) Other (please specify):

12. DOCUMENT ANNOUNCEMENT (any limitation to the bibliographic announcement of this document. This will normally correspond to the Document Availability (11). However, where further distribution (beyond the audience specified in 11) is possible, a wider announcement audience may be selected.)

Full Unlimited Announcement

13. ABSTRACT (a brief and factual summary of the document. It may also appear elsewhere in the body of the document itself. It is highly desirable that the abstract of classified documents be unclassified. Each paragraph of the abstract shall begin with an indication of the security classification of the information in the paragraph (unless the document itself is unclassified) represented as (S), (C), or (U). It is not necessary to include here abstracts in both official languages unless the text is bilingual).

Association of radar and ESM tracks is an important component for multisensor-multitarget tracking systems. It is essential to the overall performance of a track fusion process. In this report, we present an ESM/track association algorithm in a new modified polar coordinate (MPC) system. The algorithm is based on a theoretical performance analysis of ESM/radar track association techniques in the MPC. Formulas for computing the correct and false association probabilities with and without state estimation biases are derived. We also discuss the effect of the number of observable states on association performance. The proposed algorithm uses a maximum likelihood (ML) algorithm for estimating the target states, of which the observable state estimates are subsequently used for the ESM/radar track association. Computer simulations are used to demonstrate the performance and improvement of the proposed ESM/radar track association method.

14. KEYWORDS, DESCRIPTORS or IDENTIFIERS (technically meaningful terms or short phrases that characterize a document and could be helpful in cataloguing the document. They should be selected so that no security classification is required. Identifiers such as equipment model designation, trade name, military project code name, geographic location may also be included. If possible keywords should be selected from a published thesaurus. e.g. Thesaurus of Engineering and Scientific Terms (TEST) and that thesaurus-identified. If it is not possible to select indexing terms which are Unclassified, the classification of each should be indicated as with the title.)

ESM sensor, radar, bearing-only tracking, Kalman, modified polar coordinate, maximum likelihood detection and estimation, fusion, mobile sensor, tracking

Defence R&D Canada

Canada's leader in Defence
and National Security
Science and Technology

R & D pour la défense Canada

Chef de file au Canada en matière
de science et de technologie pour
la défense et la sécurité nationale

www.drdc-rddc.gc.ca